Published in final edited form as:
Neuron. 2010 September 23; 67(6): 936–952. doi:10.1016/j.neuron.2010.08.034.

Native functions of the androgen receptor are essential to pathogenesis in a *Drosophila* model of spinobulbar muscular atrophy

Natalia B. Nedelsky[1,2], **Maria Pennuto**[3], **Rebecca B. Smith**[1], **Isabella Palazzolo**[4], **Jennifer Moore**[1], **Zhiping Nie**[5], **Geoffrey Neale**[6], and **J. Paul Taylor**[1]

[1]Department of Developmental Neurobiology, St. Jude Children's Research Hospital, Memphis, TN 38105, USA

[2]Neuroscience Graduate Group, University of Pennsylvania School of Medicine, Philadelphia, PA 19104, USA

[3]Department of Neuroscience, Italian Institute of Technology, Genova 16163, Italy

[4]Neurogenetics Branch, National Institute of Neurological Disorders and Stroke, National Institutes of Health, Bethesda, MD 20892, USA

[5]Department of Neurology, University of Pennsylvania School of Medicine, Philadelphia, PA 19104, USA

[6]Hartwell Center for Bioinformatics and Biotechnology, St. Jude Children's Research Hospital, Memphis, TN 38105, USA

Summary

Spinobulbar muscular atrophy (SBMA) is a neurodegenerative disease caused by expansion of a polyglutamine tract in the androgen receptor (AR). This mutation confers toxic function to AR through unknown mechanisms. Mutant AR toxicity requires binding of its hormone ligand, suggesting that pathogenesis involves ligand-induced changes in AR. However, whether toxicity is mediated by native AR function or a novel AR function is unknown. We systematically investigated events downstream of ligand-dependent AR activation in a Drosophila model of SBMA. We show that nuclear translocation of AR is necessary but not sufficient for toxicity and that DNA binding by AR is necessary for toxicity. Mutagenesis studies demonstrated that a functional AF-2 domain is essential for toxicity, a finding corroborated by a genetic screen that identified AF-2 interactors as dominant modifiers of degeneration. These findings indicate that SBMA pathogenesis is mediated by misappropriation of native protein function, a mechanism that may apply broadly to polyglutamine diseases.

Introduction

Spinobulbar muscular atrophy (SBMA, also known as Kennedy's disease) is a progressive late-onset degenerative disorder of the motor neurons in the brainstem and spinal cord that affects only men (Kennedy et al., 1968). SBMA is a member of the polyglutamine repeat disease family, which includes at least eight other disorders, including Huntington's disease (HD), dentatorubral-pallidoluysian atrophy (DRPLA), and six forms of spinocerebellar

Correspondence should be addressed to: J. Paul Taylor, MD, PhD, Developmental Neurobiology, MS 343, D-4026, St. Jude Children's Research Hospital, 262 Danny Thomas Place, Memphis, TN 38105-3678, jpaul.taylor@stjude.org, Phone: (901) 595-6047, FAX: (901) 595-5947.
Current address of IP: Department of Neurology, Massachusetts General Hospital, Charlestown, Massachusetts 02129, USA

ataxia (SCA). All of these diseases are caused by gain-of-function mutations characterized by expanded trinucleotide (CAG) repeats in exonic regions of DNA, and all result in late-onset, progressive neurodegeneration (Zoghbi and Orr, 2000). In SBMA, the CAG repeat site is located in the androgen receptor (AR) gene and causes disease when the number of repeats is 40 or greater (La Spada et al., 1991). Patients often display signs of mild feminization, likely due to partial loss of AR function. Although loss of AR function may contribute to disease (Thomas et al., 2006), it is not sufficient for degeneration, as loss-of-function mutations to AR result in androgen insensitivity syndrome without signs of neuronal degeneration (Quigley et al., 1992).

A central mystery in the field of polyglutamine disease research arises from the observation that the same mutation in nine different proteins results in nine different diseases; yet in each disease, different subsets of neurons are affected. This pattern occurs despite widespread and overlapping expression of the disease proteins, suggesting that the inherent toxicity of the expanded polyglutamine is not the sole basis of toxicity. Indeed, in SBMA mouse models, expression of polyglutamine-expanded fragments of AR results in widespread neuronal degeneration, a phenotype that is not dissimilar from that observed in transgenic animal models expressing fragments of other polyglutamine-expanded proteins (Abel et al., 2001). In contrast, models employing full-length polyglutamine-expanded AR protein more accurately reflect the human disease, displaying restricted symptoms, lower motor neuron specificity in degeneration, and gender specificity (Chevalier-Larsen et al., 2004; Sopher et al., 2004).

These findings highlight the importance of protein context in polyglutamine disease, and raise the question of the role of protein domains other than the polyglutamine tract in toxicity. It is not clear whether the mutation results in the formation of novel, toxic interactions, or whether the mutation alters the normal, native interactions of the polyglutamine-containing protein in such a way as to result in neurotoxicity. While these possibilities are not mutually exclusive, recent studies in SCA1, SCA7, and SCA17 have provided evidence in favor of a model in which the normal function of the disease protein is tied to the mechanism of pathogenesis (Emamian et al., 2003; Friedman et al., 2007; Helmlinger et al., 2006; Lim et al., 2008; McMahon et al., 2005; Palhan et al., 2005; Tsuda et al., 2005). More direct evidence that native interactions may mediate toxicity comes from animal models in which overexpression of non-expanded ataxin-1 or AR result in pathology resembling SCA1 and SBMA, respectively (Fernandez-Funez et al., 2000; Monks et al., 2007).

In the majority of polyglutamine diseases, neither the primary function nor the native interactors of the disease proteins are well known. SBMA is an exception in that the disease protein has a well-characterized role as a ligand-dependent transcription factor. AR is a member of the nuclear hormone receptor (NHR) superfamily and resides in the cytoplasm when inactive. A number of events occur upon ligand binding, the final result of which is AR-mediated activation or repression of target genes. These ligand-induced events include several post-translational modifications, nuclear translocation, and DNA binding. These changes occur in concert with conformational changes that result in the exposure of two coregulator interaction surfaces, termed activation function-1 (AF-1) and activation function-2 (AF-2). Ligand binding to polyglutamine-expanded AR is a requisite step in disease pathogenesis. Indeed, there is now incontrovertible evidence from animal model studies as well as human studies that gender specificity in SBMA is due to higher levels of circulating androgens in males (Katsuno et al., 2002; Takeyama et al., 2002).

Although the basis of the toxic gain of function imparted by the polyglutamine expansion remains unknown, the ligand dependence of SBMA implies that ligand-induced alterations

of AR play important roles in toxicity. In this study, we used a *Drosophila* model to test the hypothesis that SBMA is mediated by ligand-induced alterations in native AR interactions. First, we present evidence that nuclear translocation of AR is necessary but not sufficient for toxicity, demonstrating that ligand-induced modifications of AR (beyond nuclear translocation) are required for pathogenesis. Second, we showed that DNA binding of polyglutamine-expanded AR is required for toxicity, indicating that the native DNA-binding function of AR is critical to pathogenesis. Third, we used a genetic screen to identify modifiers of SBMA toxicity, which revealed a pattern of AF-2-based coregulators that genetically interact with polyglutamine-expanded AR. Pursuing this finding, we show rescue of polyglutamine-expanded AR toxicity through two independent point mutations designed to disrupt the AF-2 coregulator interaction surface. To more precisely define the degenerative phenotype associated with polyglutamine-expanded AR toxicity we used expression profile analysis. This analysis confirmed that interruption of either the AF-2 or DNA binding domains robustly suppressed this molecular phenotype. In addition, analysis of the molecular phenotype of flies expressing wild-type AR revealed the same (albeit weaker) molecular phenotype as polyglutamine-expanded AR, indicating that amplification of normal AR function may underlie the toxicity of polyglutamine-expanded AR. Finally, we investigated the AR coregulator ortholog *limpet*, a gene identified in our genetic screen, as proof of principle that polyglutamine-expanded AR toxicity is mediated via native function of the AF-2 binding surface following DNA binding.

Results

Expression of polyglutamine-expanded AR in *Drosophila* results in toxicity

In order to investigate the contributions of AR interactions to polyglutamine-expanded AR toxicity, we used a *Drosophila* model of SBMA. Although human AR has no direct ortholog in flies, the NHR system is well conserved (King-Jones and Thummel, 2005). This conservation is reflected in the domain architecture of *Drosophila* nuclear receptors, including AF-1 and AF-2 coregulator interaction domains that bind to conserved motifs in nuclear receptor coregulators. It was previously demonstrated that human AR expressed in *Drosophila* tissues translocates to the nucleus in response to ligand and activates transcription of an ARE-GFP reporter transgene in response to DHT (Takeyama et al., 2002). This cross-species transactivational capacity reflects the fact that human AR interacts with endogenous *Drosophila* coactivators and corepressors; indeed, genetic modulation of *Drosophila* homologs of mammalian AR coregulators can modify the transactivational capacity of AR *in vivo* (Takeyama et al., 2004).

When human AR of varying polyglutamine lengths is expressed using the GAL4-UAS system (Brand and Perrimon, 1993), flies develop polyglutamine length- and ligand-dependent degenerative phenotypes, thus recapitulating two fundamental features of SBMA (Pandey et al., 2007; Takeyama et al., 2002). To assess toxicity in an externally visible neuronal tissue, we expressed AR in the eye using the *glass multimer reporter* driver (GMR-GAL4), which leads to transgene expression in photoreceptor neurons and accessory pigment cells in developing eye discs (Moses and Rubin, 1991). While flies expressing AR show no eye phenotype when reared on normal food, flies reared on food containing DHT exhibit a degenerative phenotype that is limited to the posterior margin of the eye (Figure 1A). The severity of the phenotype is also polyglutamine-length dependent, with AR52Q-expressing flies showing severe ommatidial pitting, disorganization, and fusion, as well as abnormal and supernumerary interommatidial bristles. In contrast, AR12Q-expressing flies show only mild ommatidial and bristle phenotypes when the transgene is expressed at equivalent levels (Figure 1A–C). Confocal imaging of eye discs confirmed that AR undergoes DHT-dependent nuclear translocation *in vivo*. This analysis also revealed diffuse

nuclear accumulation of AR and the formation of small nuclear and cytoplasmic puncta that were particularly prominent with polyglutamine-expanded AR (Figure 1D).

The polyglutamine length- and DHT-dependence of SBMA is recapitulated in several larval tissues. For example, using the larval salivary gland driver (fkh-GAL4) (Andrew et al., 2000), expression of polyglutamine-expanded AR results in a dramatic reduction of salivary gland cell size (Figure 1E–F). Larvae expressing AR in motor neurons under the control of the D42-GAL4 driver (Yeh et al., 1995) also show polyglutamine length- and DHT-dependent defects in locomotor ability as measured by larval crawling assay, indicating a significant functional deficit (Figure 1G). In addition, the number of type 1B boutons at the larval neuromuscular junction (NMJ) is significantly decreased in a DHT-dependent manner when polyglutamine-expanded AR is expressed using the motor neuron driver OK371-GAL4 (Mahr and Aberle, 2006) (Figure 1H–I).

Importantly, we noticed that expression of wild-type polyglutamine-length AR at high levels results in a degenerative phenotype that is indistinguishable from that caused by polyglutamine-expanded AR (Figure 1J–K). This is reminiscent of the SBMA-like phenotype associated with high level expression of wild-type AR in mice (Monks et al., 2007). The dose-dependent toxicity of wild-type AR suggests the possibility that amplification of native AR function may contribute to the toxicity of polyglutamine-expanded AR.

Nuclear translocation of polyglutamine-expanded AR is necessary for toxicity

The observation that ligand binding to AR is required for pathogenesis suggests a model in which non-toxic AR is converted to a proteotoxin through ligand-induced events. The first major event to occur upon ligand binding is translocation of AR to the nucleus. In most polyglutamine diseases, the primary site of cellular toxicity is thought to be the nucleus (Klement et al., 1998; Montie et al., 2009; Peters et al., 1999; Saudou et al., 1998; Takeyama et al., 2002), although cytoplasmic toxicity may also contribute (Hodgson et al., 1999; Morfini et al., 2006; Szebenyi et al., 2003). In the case of SBMA, whether nuclear translocation of polyglutamine-expanded AR is both necessary and sufficient for toxicity has not been examined *in vivo*.

AR has three major domains (Figure 2A): 1) an N-terminal transactivation domain (NTD) that contains activation function-1 (AF-1) and serves as a coregulator interaction surface, 2) a DNA-binding domain (DBD) that binds regulatory elements in AR-regulated promoters, and 3) a C-terminal ligand binding domain (LBD) that binds testosterone or dihydrotestosterone (DHT) and also harbors a second coregulator interaction surface (activation function-2, or AF-2). Bridging the DBD and LBD is a flexible hinge domain that harbors a bipartite nuclear localization sequence (NLS). To address the necessity of nuclear translocation, we generated two AR constructs designed to remain in the cytoplasm even in the presence of DHT (Figure 2A). In the first construct, we used phosphomimetic substitutions of serines 210 and 790 (AR65Q SS/DD) that prevent DHT binding to AR (Palazzolo et al., 2007). In the second construct, we mutated residues K632 and K633 (AR73Q KK/AA) in the NLS of AR; these substitutions markedly alter DHT-induced nuclear translocation (Thomas et al., 2004). COS-1 cells transfected with these constructs showed that the SS/DD and KK/AA mutations each caused AR to remain in the cytoplasm even in the presence of DHT (Figure S1A–B).

In order to investigate whether these cytoplasmic AR mutants cause toxicity *in vivo*, we generated transgenic *Drosophila* lines that express these proteins under the control of the GAL4-UAS system. We first confirmed that these modified AR proteins resist DHT-induced nuclear translocation *in vivo* in *Drosophila* by expressing the AR transgenes with

the larval salivary gland driver fkh-GAL4. Salivary glands provide an ideal model to assess subcellular localization of proteins in *Drosophila* due to their highly ordered histoarchitecture and high ratio of cytoplasm to nucleus. Using fkh-GAL4, we found that while AR52Q showed nuclear localization, AR65Q SS/DD and AR73Q KK/AA remained in the cytoplasm despite the presence of DHT in the larval medium (Figure 2C).

In order to test the toxicity of these constructs in a neuronal tissue, we next expressed the AR transgenes using GMR-GAL4. As previously shown, expression of AR52Q in the eye resulted in a degenerative phenotype in a DHT-dependent manner (Figure 2B,D). In contrast, eyes expressing AR65Q SS/DD or AR73Q KK/AA showed no degenerative phenotype even in the presence of DHT despite high expression of AR (Figure 2B,D and Figure S2A). Consistent with prior reports (Montie et al., 2009; Takeyama et al., 2002), these results indicate that nuclear translocation of polyglutamine-expanded AR is necessary for toxicity.

Nuclear translocation of polyglutamine-expanded AR is not sufficient for toxicity

In order to address whether nuclear translocation of polyglutamine-expanded AR is sufficient for toxicity, we designed AR constructs that translocate to the nucleus in a DHT-independent manner, thereby dissociating nuclear translocation from ligand binding. To this end, we fused the SV40 NLS to either the C- or N-terminus of AR (Figure 2A). As an additional control, we fused an NLS to the AR65Q SS/DD protein that is unable to bind DHT. COS-1 cells transfected with AR65Q-NLS or NLS-AR65Q SS/DD show AR localized to the nucleus even in the absence of DHT (Figure S1C–D). In addition, AR65Q-NLS retained its transactivation ability in response to DHT as measured by an ARE-luciferase reporter, though only at about 50% of AR65Q (Figure S1E). As expected, NLS-AR65Q SS/DD did not activate transcription, due to its inability to bind DHT.

We next made transgenic *Drosophila* carrying UAS-AR65Q-NLS and UAS-NLS-AR65Q SS/DD. After confirming that AR65Q-NLS and NLS-AR65Q SS/DD translocate to the nucleus in the absence of DHT *in vivo* using fkh-GAL4 (Figure 2E), we expressed these transgenes in the eye using GMR-GAL4 (Figure 2F and Figure S2B). Expression of AR65Q-NLS or NLS-AR65Q SS/DD did not cause toxicity in the absence of DHT, indicating that nuclear translocation of polyglutamine-expanded AR is not sufficient for toxicity. However, once the AR65Q-NLS animals were exposed to DHT, they developed the characteristic SBMA eye phenotype, demonstrating that DHT binding to AR provides the critical step in the conversion of polyglutamine-expanded AR from a non-toxic to a toxic molecule (Figure 2B, F).

An intact DNA-binding domain is required for polyglutamine-expanded AR toxicity

Having determined that the role of DHT in SBMA is not simply to effect translocation of AR to the nuclear compartment, but also to modify nuclear AR, we hypothesized AR's function as a DNA-binding transcription factor might play a role in pathogenesis. To investigate this hypothesis, we introduced a mutation to the AR DBD (A574D) that blocks the ability of AR to bind DNA without disrupting its ligand-binding ability (Bruggenwirth et al., 1998).

AR52Q A574D showed normal DHT-induced nuclear translocation *in vitro* (Figure S3), although transactivation capacity was severely disrupted, as predicted due to the inability of the mutated AR to bind DNA (Figure 3A). Strikingly, transgenic flies expressing AR52Q A574D using GMR-GAL4 showed no degenerative phenotype even in the presence of DHT, indicating that the A574D mutation abolished the toxicity of polyglutamine-expanded AR despite nuclear localization of AR and high transgene expression (Figure 3B–D and Figure

S2C–D). Supporting this result, flies expressing polyglutamine-expanded AR with the A574D mutation showed no larval crawling defect when AR was expressed in motor neurons (Figure 3E). Additionally, introduction of the A574D mutation resulted in salivary gland cell size that was indistinguishable from AR52Q without DHT (Figure 3F–G). These results indicate that the native DNA-binding function of AR is critical for pathogenesis.

AF-2-interacting coregulators modify the toxicity of polyglutamine-expanded AR

In the normal life cycle of AR, DNA binding is followed by the recruitment of coregulators (either corepressors or coactivators) that associate with AR at target promoters (Heinlein and Chang, 2002). We hypothesized that coregulator binding, an event immediately downstream of DNA binding, might play a role in pathogenesis.

In order to investigate the role of AR coregulators in SBMA, we performed a candidate-based genetic screen for modifiers of polyglutamine-expanded AR toxicity. We began with 73 human coregulators that are known to interact with AR. We identified 61 putative *Drosophila* orthologs of these coregulators, including 23 coactivators, 34 corepressors, and 4 coregulators with dual function. RNAi-mediated knockdown of 19/61 (31%) of these *Drosophila* coregulators dominantly modified the SBMA fly phenotype (Table 1, Figure S4A–B). These modifiers included some coregulators with obvious mechanisms of enhancement, including Pat1 and Pten, which normally function to inhibit AR nuclear translocation. The mechanism for other modifiers was less clear, although there was an interesting pattern among the hits because seven of them relate to the function of the AF-2 domain of AR. Specifically, CycD, gskt, jbug, Lmpt, Rad9, Smr, and wts (putative *Drosophila* orthologs of CCND1, GSK3B, FLNA, FHL2, RAD9, NCOR1/2, and LATS2, respectively) each plays a role in AF-2 interactions, either by binding AF-2 directly or by modifying the AF-2-based interaction with the NTD (Table 1). To confirm the specificity of these hits and to rule out off-target effects due to RNAi, we confirmed the effects of these AF-2-related hits in three additional contexts. First, we confirmed that classical alleles and aneuploid aberrations of these same genes would similarly enhance the AR52Q eye phenotype (Figure S4C). Second, after verifying that RNAi knockdown had no effect on larval crawling ability when expressed in motor neurons in the absence of AR52Q, we showed that these RNAi lines enhanced the AR52Q larval crawling defect in 6/7 cases (Table 1, Figure S4 DE). Third, we showed that the RNAi lines did not enhance the AR52Q eye phenotype nonspecifically, by crossing RNAi-expressing lines to an unrelated disease model of inclusion body myopathy associated with Paget's disease of bone and frontotemporal dementia (IBMPFD) that shows a modifiable degenerative eye phenotype (Ritson et al., 2010) (data not shown).

A functional AF-2 binding site is required for toxicity

AF-2 is a ligand-dependent hydrophobic surface flanked by opposing charged residues, K720 and E897 (Figure 4A). This surface is highly conserved across steroid hormone receptors and across species, and in most cases serves as a binding pocket for the LxxLL motifs of steroid receptor coactivator (SRC) family members (He et al., 1999). Unlike other steroid hormone receptors, however, the AF-2 of AR also binds a motif defined as FxxLF, which binds to AF-2 with higher affinity than LxxLL motifs (Dubbink et al., 2004; He et al., 2001; He et al., 2004). The FxxLF motif is found in the N-terminus of the AR, as well as in a small number of coregulators. Current models propose that AF-2 binds the NTD FxxLF motif while AR is mobile, and that the NTD/AF-2 interaction is lost upon AR binding to DNA, rendering AF-2 optimally accessible to coregulators when AR is bound to DNA (van Royen et al., 2007).

Since our targeted RNAi screen highlighted the importance of coregulator interactions with AF-2, we next investigated the role of AF-2 function in polyglutamine-expanded AR toxicity by taking advantage of three well-characterized mutations that disrupt AF-2-based interactions without influencing protein stability. The first, E897K, reverses the charge of one of the two charge clamp residues in AF-2, thereby abolishing both LxxLL- and FxxLF-mediated interactions (He et al., 1999) (Figure 4A). The second, K720A, which neutralizes the charge of the other charge clamp residue in AF-2, partially impairs AF-2 function by severely disrupting LxxLL-mediated interactions and decreasing FxxLF-based interactions by approximately 50% (Dubbink et al., 2004; He et al., 1999). The third, G21E, located two amino acids from the FxxLF sequence in the NTD, blocks the NTD/AF-2 interaction without affecting AF-2 structure (Callewaert et al., 2003). Neither E897K nor K720A alters the equilibrium binding affinity for ligand (He et al., 1999).

In COS-1 cells, AR E897K, K720A, and G21E showed DHT-induced nuclear translocation similar to wt AR (Figure S5A–B). Luciferase-based transactivation assays indicated that while K720A and G21E mutants showed unaltered transactivation capacity, the activity of AR E897K was modestly decreased (Figure 4C). When expressed *in vivo* using fkh-GAL4, we found that all three mutant proteins translocated to the nucleus in response to DHT (Figure 4B). Importantly, the AF-2 mutations E897K and K720A strongly suppressed the phenotype caused by expression of polyglutamine-expanded AR in salivary glands cells (Figure 4B and Figure S5C–D). In contrast, the G21E mutation had no impact on salivary gland phenotype (Figure 4B).

We next tested the toxicity of these mutant proteins using GMR-GAL4. We found that introduction of the E897K mutation abolished the degenerative eye phenotype, indicating that complete disruption of AF-2 binding eliminates the toxicity of polyglutamine-expanded AR despite high levels of AR expression (Figure 4E, Figure S2C–D, and Figure S5E). The K720A mutation also suppressed degeneration, confirming that LxxLL- and FxxLF-based binding to AF-2 are critical mediators of toxicity. In contrast, the G21E mutation had no discernable impact on the eye phenotype. This latter result argues that impaired coregulator interactions with AF-2, rather than impaired NTD binding to AF-2, underlie the suppressive effect of E897K and K720A mutations.

To corroborate the suppression seen by the K720A and E897K mutations, we next used the driver elav-GAL4, which drives transgene expression in all neurons. While expressing AR52Q with elav-GAL4 resulted in early larval lethality, introducing the AF-2 mutations E897K or K720A resulted in increased viability, as evidenced by more flies surviving to the pupal stage (Figure 4D and Figure S5F). When expressed in motor neurons with D42-GAL4, the E897K and K720A mutations also significantly suppressed the larval crawling defect seen in AR52Q flies (Figure 4F). In addition, AF-2 mutations suppressed the NMJ bouton phenotype, resulting in a significantly increased number of synaptic boutons, while the G21E mutation had no effect on this phenotype (Figure 4G–H). These results confirm the suppression observed in the eye while extending the findings to the cell type most affected in the human disease.

Expression profile analysis of AR mutants reveals the molecular phenotype of eye degeneration

While the rescue of eye degeneration we observe with mutations to the DNA-binding domain or AF-2 domain are robust, and we have corroborated the findings in other tissues, we felt it would be valuable to generate a molecular phenotype to serve as an objective, quantifiable assay of degeneration. Using GMR-GAL4 to drive transgene expression in the eye, we used Affymetrix arrays to profile gene expression changes in flies expressing wild-type AR, polyglutamine-expanded AR, or polyglutamine-expanded AR with mutations

affecting the DBD or AF-2. 149 genes were identified whose expression significantly changed in concert with ligand-induced degeneration in AR52Q-expressing flies, representing a molecular signature of degeneration (Figure 5A, Figure S6, and Table S1). Hierarchical cluster analysis revealed strong correlation between this molecular read-out and visual inspection of eye morphology (Figure 5A–B). Principal components analysis showed that introduction of the E897K and A574D mutations reverted the molecular phenotype back to a pattern that is indistinguishable from AR12Q or AR52Q without ligand (Figure 5C). The K720A mutation partially reversed the molecular phenotype observed in the AR52Q flies +DHT, reflecting the milder suppression observed in these eyes when scored according to the severity of their external degenerative phenotype.

For the purpose of our study, we used expression profiles as a means of quantifying eye degeneration in our model. We caution against making too much of the identity of the individual genes whose expression is changed because the molecular phenotype that accompanies eye degeneration is likely dominated by secondary gene expression changes that are a consequence rather than a cause of degeneration. Nevertheless, we recognized the possibility that embedded within these expression profiles are some gene expression changes that are primary due to AR binding. To address this possibility, we performed promoter analysis which found no evidence of enrichment of genes containing AR binding sites among the DHT-responsive gene set (data not shown). Similarly, promoter analysis showed no enrichment for genes that are responsive to endogenous nuclear hormone receptors such as the ecdysone receptor (data not shown). These results suggest that although the molecular phenotype captured by our expression profiling can be used to quantify neurodegeneration in the adult eye, secondary gene changes are likely to obscure primary gene changes that occurred in the first steps of pathogenesis.

In addition to corroborating our visual inspection with respect to E897K, A574D, and K720A mutations and toxicity, the expression profile analysis also revealed that AR12Q +DHT caused nearly the same molecular signature as AR52Q +DHT, although the degree of expression level changes was generally weaker in AR12Q compared to AR52Q (Figure 5A and Figure S6). This observation is consistent with a model in which amplification of normal AR function may underlie the toxicity of polyglutamine-expanded AR. Indeed, as described above, expression of AR12Q in fly eyes can also result in degeneration when expressed at very high levels.

Modification of the SBMA phenotype by the FxxLF-containing coregulator *limpet* is dependent on AF-2

The strong suppression observed in the E897K mutants (which eliminates FxxLF-based interactions), along with the milder suppression observed in the K720A mutants (which merely decreases FxxLF-based interactions), implicated FxxLF-based coregulator interactions as playing a significant role in toxicity. Based on our genetic screen (Table 1), we further examined the identity of our genetic modifiers in the context of FxxLF-based AF-2 interactions. Although some of these modifiers are not known to interact with AF-2 directly and not all contain FxxLF motifs, the AR coregulator four-and-a-half LIM domains 2 (FHL2, the human ortholog of *Drosophila limpet*) interacts with AF-2 directly via an FxxLF motif (Hsu et al., 2003). FHL2/limpet is well-conserved between fly and human (56.4% similarity, 74.4% identity), including the FxxLF motif (Figure S7A), and is one of a family of LIM domain-containing proteins, several of which are known to play a role in motor neuron development (Bhati et al., 2008). The exact mechanism whereby FHL2 modifies AR transactivation is unknown, although LIM domain-containing proteins have been found to act as bridging molecules between transcription factors, suggesting that they may act as scaffolds in the assembly of transcriptional complexes (Wadman et al., 1997).

Thus, *limpet* provided a good candidate for further investigation, given that it may act to positively or negatively regulate the assembly of AF-2 complexes.

We therefore performed epistasis experiments to examine the ability of *limpet* to modify the toxicity of polyglutamine-expanded AR. While RNAi knockdown of limpet in the *Drosophila* eye using GMR-GAL4 results in no externally visible phenotype in flies without the mutant AR transgene, limpet knockdown in flies expressing AR52Q enhanced the AR52Q degenerative eye phenotype (Figure 6A,C,M and Figure S7B–C). Similarly, a classical P-element allele ($Lmpt^{GE27535}$) of *limpet* enhanced the AR52Q phenotype (Figure 6B,C,M and Figure S7B). A chromosomal duplication that produces two copies of the *limpet* gene ($Dp(3;3)st^{+}g18$) (Tearle et al., 1989) suppressed the AR52Q phenotype, suggesting that depletion of limpet by AR contributes to toxicity (Figure 6C,D,M and Figure S7B). This suppression was confirmed through expression profile analysis in which we determined that 46% of the gene expression changes that accompanied ligand-dependent degeneration in AR52Q flies were completely reversed by limpet duplication (Figure 6N).

Interestingly, although genetic manipulation of *limpet* did not modify the mild phenotype of flies expressing AR12Q at moderate levels (data not shown), *limpet* alleles did modify the more severe phenotype of flies expressing AR12Q at very high levels (Figure 6E–H,M), suggesting that the molecular pathophysiology of high-expressing AR12Q flies is related to that of AR52Q flies. Importantly, limpet knockdown did not modify the phenotype of AR66Q E897K, indicating that the enhancement by limpet RNAi requires a functional AF-2 binding surface (Figure 6I–J). In addition, limpet duplication did not suppress the degenerative phenotype caused by pure polyglutamine protein (127Q) (Kazemi-Esfarjani and Benzer, 2000), demonstrating that increased levels of limpet are not globally protective, but instead show a specific genetic interaction with AR (Figure 6K–L). These results are consistent with a model in which polyglutamine-expanded AR causes toxicity through AF-2-based interactions with coregulators.

Discussion

In this study, we investigated the basis for the toxicity of polyglutamine-expanded AR by systematically interrogating ligand-dependent modifications of this nuclear hormone receptor. We showed that nuclear translocation of polyglutamine-expanded AR is necessary but not sufficient for toxicity and that DNA binding is required for toxicity. Insight from a genetic screen indicated that native interactions, those mediated by the AF-2 domain in particular, play a key role in toxicity. This suspicion was confirmed by our results indicating that toxicity is dependent upon a functional AF-2 binding surface. Specifically, we demonstrated that K720A and E897K mutations to the AF-2 coregulator interaction surface attenuated polyglutamine-expanded AR toxicity, while interruption of the NTD/AF-2 interaction had no effect. In the majority of assays, the E897K mutation resulted in a stronger suppression than K720A (Figure 4D–E, G–H), an observation that is consistent with the stronger AF-2 disruption due the reversal of charge (E/K) compared to the neutralization of charge (K/A). These results indicate that AF-2 function is essential for polyglutamine-expanded AR toxicity. Importantly, the morphological (Figure 1J) and molecular (Figure 5) phenotypes of AR12Q recapitulate those of AR52Q, only less strongly, suggesting that polyglutamine-expanded AR toxicity may be mediated by amplification of wild-type AR function. We conclude that SBMA pathogenesis is mediated by amplification of native AR interactions, and that functions of the AF-2 domain are essential to toxicity.

Although we have demonstrated that polyglutamine-expanded AR toxicity requires DNA binding followed by association with AF-2 coregulators, we do not yet know how this results in toxicity. We favor a model in which the AF-2 domain of AR competes with other

transcription factors for a finite supply of coregulators. According to this model, amplification of AR activity could result in reduced availability of coregulators for important functions. This model is consistent with our observation that RNAi-mediated knockdown of AF-2 interactors consistently enhances toxicity. A key outstanding question not answered in this study is how AR activity in the nucleus is amplified. One possibility is that aggregation-prone polyglutamine-expanded AR adopts a toxic conformation that amplifies AF-2-based interactions. However, the fact that we did not detect polyglutamine length-dependent changes in co-immunoprecipitation of AR and FHL2 argues against this possibility (Figure S8). An alternative possibility is that polyglutamine expansion amplifies AR activity (and AF-2 function in particular) independent of any change in the intrinsic ability of AR to interact with coregulators. For example, by reducing the inactivation rate of DNA-bound AR or by reducing the rate of AR nuclear efflux similar to what has been observed for ataxin-7 (Taylor et al., 2006). The mechanism by which polyglutamine expansion amplifies AR nuclear activity will be an important focus for future studies. Previous analysis has revealed the presence of high molecular weight species of presumed aggregated polyglutamine-expanded AR in our *Drosophila* model of SBMA (Pandey et al., 2007). These species are also present in the mutant forms of AR included in the current study. Quantitative analysis shows no correlation between the amount of high molecular weight species and neurodegeneration in this *Drosophila* model (Figure S2 E–F). While this observation is intriguing, thorough assessment of the relative contributions of aggregation and altered native function will require follow up studies in mammals.

While our results indicate that AF-2 function is essential to toxicity (Figure 7), it is likely that multiple native interactions influence the toxicity of polyglutamine-expanded AR, and this is substantiated by the results of our genetic screen. For example, AF-1-interacting coregulators Hey and Rbf were found to modify toxicity, indicating that coregulator interactions at AF-1 likely participate in pathogenesis. One AF-1-interacting protein identified in our screen, Rbf, (the *Drosophila* ortholog of Rb, or Retinoblastoma protein) was also recently shown to modulate the toxicity of polyglutamine-expanded AR in another *Drosophila* model of SBMA. In this study, Rb was shown to have increased association with polyglutamine-expanded AR, leading to reduced Rb activity and subsequent loss of regulation of Rb-associated genes (Suzuki et al., 2009). Such a model may also apply to AF-2-based interactions.

These observations may easily be aligned with recent reports relating to three other polyglutamine diseases in which the data point away from the intrinsic toxicity of expanded polyglutamine and toward the toxic consequences of amplified native interactions. A series of publications from the Orr and Zoghbi labs has illuminated the role of native interactions of ataxin-1 in the pathogenesis of SCA1 (Emamian et al., 2003; Lim et al., 2008; Tsuda et al., 2005). Specifically, polyglutamine expansion favors interaction with the RNA-binding protein RBM17, contributing to SCA1 neuropathology through a gain-of-function mechanism. Concomitantly, polyglutamine expansion attenuates interaction with Capicua, contributing to SCA1 through a partial loss-of-function mechanism (Lim et al., 2008). Analogous mechanisms have been implicated in the pathogenesis of SCA7 and SCA17, although less is known about the identity of the native interactions that are key to pathogenesis (Friedman et al., 2007; Helmlinger et al., 2006; McMahon et al., 2005; Palhan et al., 2005).

While the AF-2 result is interesting insofar as it highlights a model in which polyglutamine expansion drives toxicity through native function, the greatest significance is that these results reveal an opportunity for therapeutic intervention. An entire therapeutic enterprise has developed around targeting of AF-2/coregulator interactions with small molecules in efforts to combat prostate cancer, hyperandrogenic syndromes and male-pattern baldness

among others (Chang and McDonnell, 2005; Schapira, 2002). Indeed, the drug ASC-J9 was found to ameliorate neurodegeneration in a mouse model of SBMA and this was attributed to increased degradation of polyglutamine-expanded AR (Yang et al., 2007). However, in light of our findings it is worth noting that ASC-J9 disrupts the interaction between the AF-2 interactions with FxxLF-containing coregulators, suggesting that the beneficial effect of ASC-J9 may represent targeted interruption of AF-2-based interactions that are essential mediators of toxicity (Ohtsu et al., 2002). Although further studies are required to replicate these results in a mammalian model, our current findings allow for the possibility that SBMA patients will not have to rely on drugs that result in global androgen deprivation, but instead hope for therapeutic agents that will act in motor neurons to specifically target toxic AR interactions.

Experimental Procedures

Antibodies

Primary antibodies used: AR (N20, Santa Cruz Biotechnology), actin (I-19-R, Santa Cruz Biotechnology), α-tubulin (T5168, Sigma), FLAG (M2 F1804, Sigma), Anti-HRP-Cy3 conjugate (Jackson Immunoresearch), Discs-Large (DSHB 4F3). Secondary antibodies used for biochemistry: IRDye 800CW Goat Anti-Mouse IgG, IRDye 680 Goat Anti-Mouse IgG, IRDye 680 Goat Anti-Rabbit IgG, IRDye 800CW Goat Anti-Rabbit IgG (Li-Cor Biosciences). For *in vivo* staining: Goat anti-mouse Alexa Fluor 488 (Invitrogen), Goat anti-rabbit Alexa Fluor 488 (Invitrogen), FITC anti-rabbit (Jackson ImmunoResearch). The mouse anti-Discs-Large hybridoma antibody developed by Corey Goodman was obtained from the Developmental Studies Hybridoma Bank developed under the auspices of the NICHD and maintained by the University of Iowa, Department of Biology, Iowa City, IA 52242.

Cloning

Mutagenesis (G21E, S210D, A574D, K720A, S790D, and E879K) was performed using Quikchange II XL Mutagenesis Kit (Stratagene). NLS sequences were added to AR using a PCR-based method.

Eye disc staining

UAS-AR flies were crossed to GMR-GAL4 flies on food with or without 1 mM DHT (Steraloids). Pupal eye discs were dissected and fixed with 4% PFA for 30 minutes at room temperature. Discs were stained with primary antibody for 16 hours at 4°C and secondary antibody for 1 hour at room temperature. Phalloidin staining (Alexa Fluor568 Phalloidin, Invitrogen) was performed for 2 hours at room temperature. Discs were washed and embedded using Glycergel (Dako), mounted, and examined by laser scanning confocal microscopy.

Eye phenotypes

UAS-AR flies were crossed to GMR-GAL4 flies at 25°C or 29°C on food containing either 1 mM DHT (Steraloids) or 1% ethanol. Eye phenotypes of anesthetized female flies were evaluated with a Leica MZ APO or M205C stereomicroscope and photographed with a Leica DFC320 digital camera. Blinded scoring of the AR phenotype was performed as previously described (Pandey et al., 2007).

Fly stocks

Mutant AR flies were generated by cloning human AR constructs into pUAST. DNA was injected into w^{1118} embryos by BestGene Inc (Chino Hills, CA). At least 4 independently

generated transgenic lines were evaluated for all AR-expressing flies. Classical alleles and deficiency lines (Df(1)sd72b, Df(3R)tll-e, Df(2R)Exel6079, Df(3L)Cat, Df(1)N105, wts[3–17], $Lmpt^{GE27535}$, and Dp(3;3)st+g18) were obtained from Bloomington Stock Center (Bloomington, IN). RNAi transgenic lines were obtained from the Vienna *Drosophila* RNAi Center (Vienna, Austria).

Larval crawling

UAS-AR flies were crossed to D42-GAL4 flies at 25°C on food containing either 1 mM DHT or 1% ethanol. Larval crawling was performed on a 1% agarose gel in a 245 mm^2 dish with gridlines spaced by 2.5 mm. Wandering third instar larvae were allowed to acclimate for 5 minutes, and the number of gridlines passed by the posterior end of the larvae in 30 seconds was counted. Each larva was tested 3 times.

Luciferase assays

Luciferase assays were performed in HEK293T cells as previously described (Palazzolo et al., 2007). Briefly, cells were transfected with indicated AR constructs together with both the luciferase pARE-E1b-Luc and the β-galactosidase pCMV β reporter constructs. AR transactivation was measured in the presence and absence of DHT by luciferase assay and normalized to β-galactosidase activity.

Microarray gene expression profiling analysis

UAS-AR flies were crossed to GMR-GAL4 flies at 29°C on food containing either 1 mM DHT (Steraloids) or 1% ethanol. Heads of 15 female offspring were collected, frozen, and RNA was extracted using TRIzol (Invitrogen). Details of processing and analysis may be found in Supplemental Information.

Neuromuscular bouton counting

UAS-AR flies were crossed to OK371-GAL4 flies at 25°C on food containing either 1 mM DHT (Steraloids) or 1% ethanol. Third instar larvae were heat killed, dissected in PBS, and fixed with 4% PFA for 20 minutes. Primary antibody staining was performed at 4°C overnight and secondary antibody staining was performed at room temperature for 4 hours. After staining, pelts were mounted in Fluoromount-G (SouthernBiotech). Boutons at muscle 4 segments A2-A5 on the right and left side were quantified in the mounted muscle preparations.

RNAi screen

The list of 73 AR-interacting coregulators was generated through literature review. Orthology prediction for *Drosophila* orthologs of these coregulators was performed using the HUGO Gene Nomenclature Committee Comparison of Orthology Prediction tool along with PSI-BLAST. RNAi lines were obtained from the Vienna *Drosophila* RNAi Center. Flies expressing UAS-RNAi were crossed to flies expressing GMR-GAL4; UAS-AR52Q at 29°C on food containing either 1 mM DHT (Steraloids) or 1% ethanol. Eye phenotypes of anesthetized female flies were evaluated with a Leica MZ APO or M205C stereomicroscope and photographed with a Leica DFC320 digital camera.

Salivary gland staining

UAS-AR flies were crossed to fkh-GAL4 flies at 25°C on food containing either 1 mM DHT (Steraloids) or 1% ethanol. For antibody staining, wandering third instar larvae were collected and salivary glands were dissected into 4% PFA in PBS. Glands were stained with primary antibody for 16 hours at 4°C and secondary antibody for 2 hours at room temperature. For details of fixation and washing, see Supplemental Information. For

phalloidin staining, wandering third instar larvae were collected and salivary glands were dissected and stained as previously described (Martin and Baehrecke, 2004) using Texas Red-Phalloidin (Invitrogen). Slides were examined using a Leica DMIRE2 microscope and cell size was determined using phalloidin staining and Slidebook software (Intelligent Imaging Innovations).

Statistics

Statistical comparisons were performed by ANOVA and Tukey HSD Test or Student's t-test as appropriate.

Viability

UAS-AR flies were crossed to elav-GAL4 flies at 25°C on food containing either 1 mM DHT (Steraloids) or 1% ethanol. Crosses were set up using 1 female and 1 male. The number of pupae on the sides of the vial and the surface of the food were counted 16 days after parents were added.

Western blotting

UAS-AR flies were crossed to GMR-GAL4 flies at 29°C. Heads of 3 female offspring were collected, frozen, and lysed in RIPA buffer (150 mM NaCl, 6 mM Na_2HPO_4, 4 mM NaH_2PO_4, 2 mM EDTA, 1% NaDOC, 1% Triton X-100, 0.1% SDS) with protease inhibitors (Roche). The lysate was sonicated, boiled, and run on 7.5% Tris-HCl SDS-PAGE gels (Bio-Rad). Proteins were transferred to nitrocellulose membranes (GE Healthcare) and immunoblotted. Blots were developed using the Odyssey Imaging System (Li-Cor Biosciences).

Supplementary Material

Refer to Web version on PubMed Central for supplementary material.

Acknowledgments

We thank Eric Baehrecke, Christina McPhee, Yakup Batlevi, and Kevin Cook for technical advice and reagents. Drosophila anti-lamin antibody (mAb-ADL 84) was a gift from Paul Fisher, SUNY Stonybrook. FLAG-FHL2 DNA was a gift from Christopher Mack, University of North Carolina. NLS-AR24Q was a gift from Bryce Paschal, University of Virginia. We thank Andrew Lieberman for KK/AA DNA. We also thank Rita Balice-Gordon, Thomas Jongens, Robert Kalb, and Taylor lab members for helpful comments. Financial support was provided by the Muscular Dystrophy Association, the Kennedy's Disease Association, NIH grant NS053825, and ALSAC (American Lebanese Syrian Associated Charities).

References

Abel A, Walcott J, Woods J, Duda J, Merry DE. Expression of expanded repeat androgen receptor produces neurologic disease in transgenic mice. Hum Mol Genet. 2001; 10:107–116. [PubMed: 11152658]

Andrew DJ, Henderson KD, Seshaiah P. Salivary gland development in Drosophila melanogaster. Mech Dev. 2000; 92:5–17. [PubMed: 10704884]

Belandia B, Powell SM, Garcia-Pedrero JM, Walker MM, Bevan CL, Parker MG. Hey1, a mediator of notch signaling, is an androgen receptor corepressor. Mol Cell Biol. 2005; 25:1425–1436. [PubMed: 15684393]

Bhati M, Lee C, Nancarrow AL, Lee M, Craig VJ, Bach I, Guss JM, Mackay JP, Matthews JM. Implementing the LIM code: the structural basis for cell type-specific assembly of LIM-homeodomain complexes. EMBO J. 2008; 27:2018–2029. [PubMed: 18583962]

Brand AH, Perrimon N. Targeted gene expression as a means of altering cell fates and generating dominant phenotypes. Development. 1993; 118:401–415. [PubMed: 8223268]

Bruggenwirth HT, Boehmer AL, Lobaccaro JM, Chiche L, Sultan C, Trapman J, Brinkmann AO. Substitution of Ala564 in the first zinc cluster of the deoxyribonucleic acid (DNA)-binding domain of the androgen receptor by Asp, Asn, or Leu exerts differential effects on DNA binding. Endocrinology. 1998; 139:103–110. [PubMed: 9421404]

Burd CJ, Petre CE, Moghadam H, Wilson EM, Knudsen KE. Cyclin D1 binding to the androgen receptor (AR) NH2-terminal domain inhibits activation function 2 association and reveals dual roles for AR corepression. Mol Endocrinol. 2005; 19:607–620. [PubMed: 15539430]

Callewaert L, Verrijdt G, Christiaens V, Haelens A, Claessens F. Dual function of an amino-terminal amphipatic helix in androgen receptor-mediated transactivation through specific and nonspecific response elements. J Biol Chem. 2003; 278:8212–8218. [PubMed: 12509416]

Chang CY, McDonnell DP. Androgen receptor-cofactor interactions as targets for new drug discovery. Trends Pharmacol Sci. 2005; 26:225–228. [PubMed: 15860367]

Chen G, Nomura M, Morinaga H, Matsubara E, Okabe T, Goto K, Yanase T, Zheng H, Lu J, Nawata H. Modulation of androgen receptor transactivation by FoxH1. A newly identified androgen receptor corepressor. J Biol Chem. 2005; 280:36355–36363. [PubMed: 16120611]

Chevalier-Larsen ES, O'Brien CJ, Wang H, Jenkins SC, Holder L, Lieberman AP, Merry DE. Castration restores function and neurofilament alterations of aged symptomatic males in a transgenic mouse model of spinal and bulbar muscular atrophy. J Neurosci. 2004; 24:4778–4786. [PubMed: 15152038]

Dubbink HJ, Hersmus R, Verma CS, van der Korput HA, Berrevoets CA, van Tol J, Ziel-van der Made AC, Brinkmann AO, Pike AC, Trapman J. Distinct recognition modes of FXXLF and LXXLL motifs by the androgen receptor. Mol Endocrinol. 2004; 18:2132–2150. [PubMed: 15178743]

Emamian ES, Kaytor MD, Duvick LA, Zu T, Tousey SK, Zoghbi HY, Clark HB, Orr HT. Serine 776 of ataxin-1 is critical for polyglutamine-induced disease in SCA1 transgenic mice. Neuron. 2003; 38:375–387. [PubMed: 12741986]

Fernandez-Funez P, Nino-Rosales ML, de Gouyon B, She WC, Luchak JM, Martinez P, Turiegano E, Benito J, Capovilla M, Skinner PJ, et al. Identification of genes that modify ataxin-1-induced neurodegeneration. Nature. 2000; 408:101–106. [PubMed: 11081516]

Friedman MJ, Shah AG, Fang ZH, Ward EG, Warren ST, Li S, Li XJ. Polyglutamine domain modulates the TBP-TFIIB interaction: implications for its normal function and neurodegeneration. Nat Neurosci. 2007; 10:1519–1528. [PubMed: 17994014]

Hayes SA, Zarnegar M, Sharma M, Yang F, Peehl DM, ten Dijke P, Sun Z. SMAD3 represses androgen receptor-mediated transcription. Cancer Res. 2001; 61:2112–2118. [PubMed: 11280774]

He B, Bowen NT, Minges JT, Wilson EM. Androgen-induced NH2- and COOH-terminal Interaction Inhibits p160 coactivator recruitment by activation function 2. J Biol Chem. 2001; 276:42293–42301. [PubMed: 11551963]

He B, Gampe RT Jr, Kole AJ, Hnat AT, Stanley TB, An G, Stewart EL, Kalman RI, Minges JT, Wilson EM. Structural basis for androgen receptor interdomain and coactivator interactions suggests a transition in nuclear receptor activation function dominance. Mol Cell. 2004; 16:425–438. [PubMed: 15525515]

He B, Kemppainen JA, Voegel JJ, Gronemeyer H, Wilson EM. Activation function 2 in the human androgen receptor ligand binding domain mediates interdomain communication with the NH(2)-terminal domain. J Biol Chem. 1999; 274:37219–37225. [PubMed: 10601285]

Heinlein CA, Chang C. Androgen receptor (AR) coregulators: an overview. Endocr Rev. 2002; 23:175–200. [PubMed: 11943742]

Helmlinger D, Hardy S, Abou-Sleymane G, Eberlin A, Bowman AB, Gansmuller A, Picaud S, Zoghbi HY, Trottier Y, Tora L, Devys D. Glutamine-expanded ataxin-7 alters TFTC/STAGA recruitment and chromatin structure leading to photoreceptor dysfunction. PLoS Biol. 2006; 4:e67. [PubMed: 16494529]

Hodgson JG, Agopyan N, Gutekunst CA, Leavitt BR, LePiane F, Singaraja R, Smith DJ, Bissada N, McCutcheon K, Nasir J, et al. A YAC mouse model for Huntington's disease with full-length mutant huntingtin, cytoplasmic toxicity, and selective striatal neurodegeneration. Neuron. 1999; 23:181–192. [PubMed: 10402204]

Hsu CL, Chen YL, Yeh S, Ting HJ, Hu YC, Lin H, Wang X, Chang C. The use of phage display technique for the isolation of androgen receptor interacting peptides with (F/W)XXL(F/W) and FXXLY new signature motifs. J Biol Chem. 2003; 278:23691–23698. [PubMed: 12714604]

Katsuno M, Adachi H, Kume A, Li M, Nakagomi Y, Niwa H, Sang C, Kobayashi Y, Doyu M, Sobue G. Testosterone reduction prevents phenotypic expression in a transgenic mouse model of spinal and bulbar muscular atrophy. Neuron. 2002; 35:843–854. [PubMed: 12372280]

Kazemi-Esfarjani P, Benzer S. Genetic suppression of polyglutamine toxicity in Drosophila. Science. 2000; 287:1837–1840. [PubMed: 10710314]

Kennedy WR, Alter M, Sung JH. Progressive proximal spinal and bulbar muscular atrophy of late onset. A sex-linked recessive trait. Neurology. 1968; 18:671–680. [PubMed: 4233749]

King-Jones K, Thummel CS. Nuclear receptors--a perspective from Drosophila. Nat Rev Genet. 2005; 6:311–323. [PubMed: 15803199]

Klement IA, Skinner PJ, Kaytor MD, Yi H, Hersch SM, Clark HB, Zoghbi HY, Orr HT. Ataxin-1 nuclear localization and aggregation: role in polyglutamine-induced disease in SCA1 transgenic mice. Cell. 1998; 95:41–53. [PubMed: 9778246]

La Spada AR, Wilson EM, Lubahn DB, Harding AE, Fischbeck KH. Androgen receptor gene mutations in X-linked spinal and bulbar muscular atrophy. Nature. 1991; 352:77–79. [PubMed: 2062380]

Lee YF, Shyr CR, Thin TH, Lin WJ, Chang C. Convergence of two repressors through heterodimer formation of androgen receptor and testicular orphan receptor-4: a unique signaling pathway in the steroid receptor superfamily. Proc Natl Acad Sci U S A. 1999; 96:14724–14729. [PubMed: 10611280]

Liao G, Chen LY, Zhang A, Godavarthy A, Xia F, Ghosh JC, Li H, Chen JD. Regulation of androgen receptor activity by the nuclear receptor corepressor SMRT. J Biol Chem. 2003; 278:5052–5061. [PubMed: 12441355]

Lim J, Crespo-Barreto J, Jafar-Nejad P, Bowman AB, Richman R, Hill DE, Orr HT, Zoghbi HY. Opposing effects of polyglutamine expansion on native protein complexes contribute to SCA1. Nature. 2008; 452:713–718. [PubMed: 18337722]

Lin HK, Hu YC, Lee DK, Chang C. Regulation of androgen receptor signaling by PTEN (phosphatase and tensin homolog deleted on chromosome 10) tumor suppressor through distinct mechanisms in prostate cancer cells. Mol Endocrinol. 2004; 18:2409–2423. [PubMed: 15205473]

Loy CJ, Sim KS, Yong EL. Filamin-A fragment localizes to the nucleus to regulate androgen receptor and coactivator functions. Proc Natl Acad Sci U S A. 2003; 100:4562–4567. [PubMed: 12682292]

Mahr A, Aberle H. The expression pattern of the Drosophila vesicular glutamate transporter: a marker protein for motoneurons and glutamatergic centers in the brain. Gene Expr Patterns. 2006; 6:299–309. [PubMed: 16378756]

Martin DN, Baehrecke EH. Caspases function in autophagic programmed cell death in Drosophila. Development. 2004; 131:275–284. [PubMed: 14668412]

McMahon SJ, Pray-Grant MG, Schieltz D, Yates JR 3rd, Grant PA. Polyglutamine-expanded spinocerebellar ataxia-7 protein disrupts normal SAGA and SLIK histone acetyltransferase activity. Proc Natl Acad Sci U S A. 2005; 102:8478–8482. [PubMed: 15932941]

Monks DA, Johansen JA, Mo K, Rao P, Eagleson B, Yu Z, Lieberman AP, Breedlove SM, Jordan CL. Overexpression of wild-type androgen receptor in muscle recapitulates polyglutamine disease. Proc Natl Acad Sci U S A. 2007; 104:18259–18264. [PubMed: 17984063]

Montie HL, Cho MS, Holder L, Liu Y, Tsvetkov AS, Finkbeiner S, Merry DE. Cytoplasmic retention of polyglutamine-expanded androgen receptor ameliorates disease via autophagy in a mouse model of spinal and bulbar muscular atrophy. Hum Mol Genet. 2009; 18:1937–1950. [PubMed: 19279159]

Morfini G, Pigino G, Szebenyi G, You Y, Pollema S, Brady ST. JNK mediates pathogenic effects of polyglutamine-expanded androgen receptor on fast axonal transport. Nat Neurosci. 2006; 9:907–916. [PubMed: 16751763]

Moses K, Rubin GM. Glass encodes a site-specific DNA-binding protein that is regulated in response to positional signals in the developing Drosophila eye. Genes Dev. 1991; 5:583–593. [PubMed: 2010085]

Muller JM, Isele U, Metzger E, Rempel A, Moser M, Pscherer A, Breyer T, Holubarsch C, Buettner R, Schule R. FHL2, a novel tissue-specific coactivator of the androgen receptor. EMBO J. 2000; 19:359–369. [PubMed: 10654935]

Ohtsu H, Xiao Z, Ishida J, Nagai M, Wang HK, Itokawa H, Su CY, Shih C, Chiang T, Chang E, et al. Antitumor agents. 217. Curcumin analogues as novel androgen receptor antagonists with potential as anti-prostate cancer agents. J Med Chem. 2002; 45:5037–5042. [PubMed: 12408714]

Palazzolo I, Burnett BG, Young JE, Brenne PL, La Spada AR, Fischbeck KH, Howell BW, Pennuto M. Akt blocks ligand binding and protects against expanded polyglutamine androgen receptor toxicity. Hum Mol Genet. 2007; 16:1593–1603. [PubMed: 17470458]

Palhan VB, Chen S, Peng GH, Tjernberg A, Gamper AM, Fan Y, Chait BT, La Spada AR, Roeder RG. Polyglutamine-expanded ataxin-7 inhibits STAGA histone acetyltransferase activity to produce retinal degeneration. Proc Natl Acad Sci U S A. 2005; 102:8472–8477. [PubMed: 15932940]

Palvimo JJ, Reinikainen P, Ikonen T, Kallio PJ, Moilanen A, Janne OA. Mutual transcriptional interference between RelA and androgen receptor. J Biol Chem. 1996; 271:24151–24156. [PubMed: 8798655]

Pandey UB, Nie Z, Batlevi Y, McCray BA, Ritson GP, Nedelsky NB, Schwartz SL, DiProspero NA, Knight MA, Schuldiner O, et al. HDAC6 rescues neurodegeneration and provides an essential link between autophagy and the UPS. Nature. 2007; 447:859–863. [PubMed: 17568747]

Peters MF, Nucifora FC Jr, Kushi J, Seaman HC, Cooper JK, Herring WJ, Dawson VL, Dawson TM, Ross CA. Nuclear targeting of mutant Huntingtin increases toxicity. Mol Cell Neurosci. 1999; 14:121–128. [PubMed: 10479410]

Powzaniuk M, McElwee-Witmer S, Vogel RL, Hayami T, Rutledge SJ, Chen F, Harada S, Schmidt A, Rodan GA, Freedman LP, Bai C. The LATS2/KPM tumor suppressor is a negative regulator of the androgen receptor. Mol Endocrinol. 2004; 18:2011–2023. [PubMed: 15131260]

Quigley CA, Friedman KJ, Johnson A, Lafreniere RG, Silverman LM, Lubahn DB, Brown TR, Wilson EM, Willard HF, French FS. Complete deletion of the androgen receptor gene: definition of the null phenotype of the androgen insensitivity syndrome and determination of carrier status. J Clin Endocrinol Metab. 1992; 74:927–933. [PubMed: 1347772]

Ritson GP, Custer SK, Freibaum BD, Guinto JB, Geffel D, Moore J, Tang W, Winton MJ, Neumann M, Trojanowski JQ, et al. TDP-43 mediates degeneration in a novel Drosophila model of disease caused by mutations in VCP/p97. J Neurosci. 2010; 30:7729–7739. [PubMed: 20519548]

Saudou F, Finkbeiner S, Devys D, Greenberg ME. Huntingtin acts in the nucleus to induce apoptosis but death does not correlate with the formation of intranuclear inclusions. Cell. 1998; 95:55–66. [PubMed: 9778247]

Schapira M. Pharmacogenomics opportunities in nuclear receptor targeted cancer therapy. Curr Cancer Drug Targets. 2002; 2:243–256. [PubMed: 12188910]

Schneikert J, Peterziel H, Defossez PA, Klocker H, Launoit Y, Cato AC. Androgen receptor-Ets protein interaction is a novel mechanism for steroid hormone-mediated down-modulation of matrix metalloproteinase expression. J Biol Chem. 1996; 271:23907–23913. [PubMed: 8798622]

Sopher BL, Thomas PS Jr, LaFevre-Bernt MA, Holm IE, Wilke SA, Ware CB, Jin LW, Libby RT, Ellerby LM, La Spada AR. Androgen receptor YAC transgenic mice recapitulate SBMA motor neuronopathy and implicate VEGF164 in the motor neuron degeneration. Neuron. 2004; 41:687–699. [PubMed: 15003169]

Suzuki E, Zhao Y, Ito S, Sawatsubashi S, Murata T, Furutani T, Shirode Y, Yamagata K, Tanabe M, Kimura S, et al. Aberrant E2F activation by polyglutamine expansion of androgen receptor in SBMA neurotoxicity. Proc Natl Acad Sci U S A. 2009; 106:3818–3822. [PubMed: 19237573]

Szebenyi G, Morfini GA, Babcock A, Gould M, Selkoe K, Stenoien DL, Young M, Faber PW, MacDonald ME, McPhaul MJ, Brady ST. Neuropathogenic forms of huntingtin and androgen receptor inhibit fast axonal transport. Neuron. 2003; 40:41–52. [PubMed: 14527432]

Takeyama K, Ito S, Sawatsubashi S, Shirode Y, Yamamoto A, Suzuki E, Maki A, Yamagata K, Zhao Y, Kouzmenko A, et al. A novel genetic system for analysis of co-activators for the N-terminal transactivation function domain of the human androgen receptor. Biosci Biotechnol Biochem. 2004; 68:1209–1215. [PubMed: 15215582]

Takeyama K, Ito S, Yamamoto A, Tanimoto H, Furutani T, Kanuka H, Miura M, Tabata T, Kato S. Androgen-dependent neurodegeneration by polyglutamine-expanded human androgen receptor in Drosophila. Neuron. 2002; 35:855–864. [PubMed: 12372281]

Taylor J, Grote SK, Xia J, Vandelft M, Graczyk J, Ellerby LM, La Spada AR, Truant R. Ataxin-7 can export from the nucleus via a conserved exportin-dependent signal. J Biol Chem. 2006; 281:2730–2739. [PubMed: 16314424]

Tearle RG, Belote JM, McKeown M, Baker BS, Howells AJ. Cloning and characterization of the scarlet gene of Drosophila melanogaster. Genetics. 1989; 122:595–606. [PubMed: 2503416]

Thomas M, Dadgar N, Aphale A, Harrell JM, Kunkel R, Pratt WB, Lieberman AP. Androgen receptor acetylation site mutations cause trafficking defects, misfolding, and aggregation similar to expanded glutamine tracts. J Biol Chem. 2004; 279:8389–8395. [PubMed: 14670946]

Thomas PS Jr, Fraley GS, Damian V, Woodke LB, Zapata F, Sopher BL, Plymate SR, La Spada AR. Loss of endogenous androgen receptor protein accelerates motor neuron degeneration and accentuates androgen insensitivity in a mouse model of X-linked spinal and bulbar muscular atrophy. Hum Mol Genet. 2006; 15:2225–2238. [PubMed: 16772330]

Tsuda H, Jafar-Nejad H, Patel AJ, Sun Y, Chen HK, Rose MF, Venken KJ, Botas J, Orr HT, Bellen HJ, Zoghbi HY. The AXH domain of Ataxin-1 mediates neurodegeneration through its interaction with Gfi-1/Senseless proteins. Cell. 2005; 122:633–644. [PubMed: 16122429]

van Royen ME, Cunha SM, Brink MC, Mattern KA, Nigg AL, Dubbink HJ, Verschure PJ, Trapman J, Houtsmuller AB. Compartmentalization of androgen receptor protein-protein interactions in living cells. J Cell Biol. 2007; 177:63–72. [PubMed: 17420290]

Wadman IA, Osada H, Grutz GG, Agulnick AD, Westphal H, Forster A, Rabbitts TH. The LIM-only protein Lmo2 is a bridging molecule assembling an erythroid, DNA-binding complex which includes the TAL1, E47, GATA-1 and Ldb1/NLI proteins. EMBO J. 1997; 16:3145–3157. [PubMed: 9214632]

Wang L, Hsu CL, Ni J, Wang PH, Yeh S, Keng P, Chang C. Human checkpoint protein hRad9 functions as a negative coregulator to repress androgen receptor transactivation in prostate cancer cells. Mol Cell Biol. 2004a; 24:2202–2213. [PubMed: 14966297]

Wang L, Lin HK, Hu YC, Xie S, Yang L, Chang C. Suppression of androgen receptor-mediated transactivation and cell growth by the glycogen synthase kinase 3 beta in prostate cells. J Biol Chem. 2004b; 279:32444–32452. [PubMed: 15178691]

Yang Z, Chang YJ, Yu IC, Yeh S, Wu CC, Miyamoto H, Merry DE, Sobue G, Chen LM, Chang SS, Chang C. ASC-J9 ameliorates spinal and bulbar muscular atrophy phenotype via degradation of androgen receptor. Nat Med. 2007; 13:348–353. [PubMed: 17334372]

Yeh E, Gustafson K, Boulianne GL. Green fluorescent protein as a vital marker and reporter of gene expression in Drosophila. Proc Natl Acad Sci U S A. 1995; 92:7036–7040. [PubMed: 7624365]

Yeh S, Miyamoto H, Nishimura K, Kang H, Ludlow J, Hsiao P, Wang C, Su C, Chang C. Retinoblastoma, a tumor suppressor, is a coactivator for the androgen receptor in human prostate cancer DU145 cells. Biochem Biophys Res Commun. 1998; 248:361–367. [PubMed: 9675141]

Yu X, Li P, Roeder RG, Wang Z. Inhibition of androgen receptor-mediated transcription by amino-terminal enhancer of split. Mol Cell Biol. 2001; 21:4614–4625. [PubMed: 11416139]

Zhang Y, Yang Y, Yeh S, Chang C. ARA67/PAT1 functions as a repressor to suppress androgen receptor transactivation. Mol Cell Biol. 2004; 24:1044–1057. [PubMed: 14729952]

Zoghbi HY, Orr HT. Glutamine repeats and neurodegeneration. Annu Rev Neurosci. 2000; 23:217–247. [PubMed: 10845064]

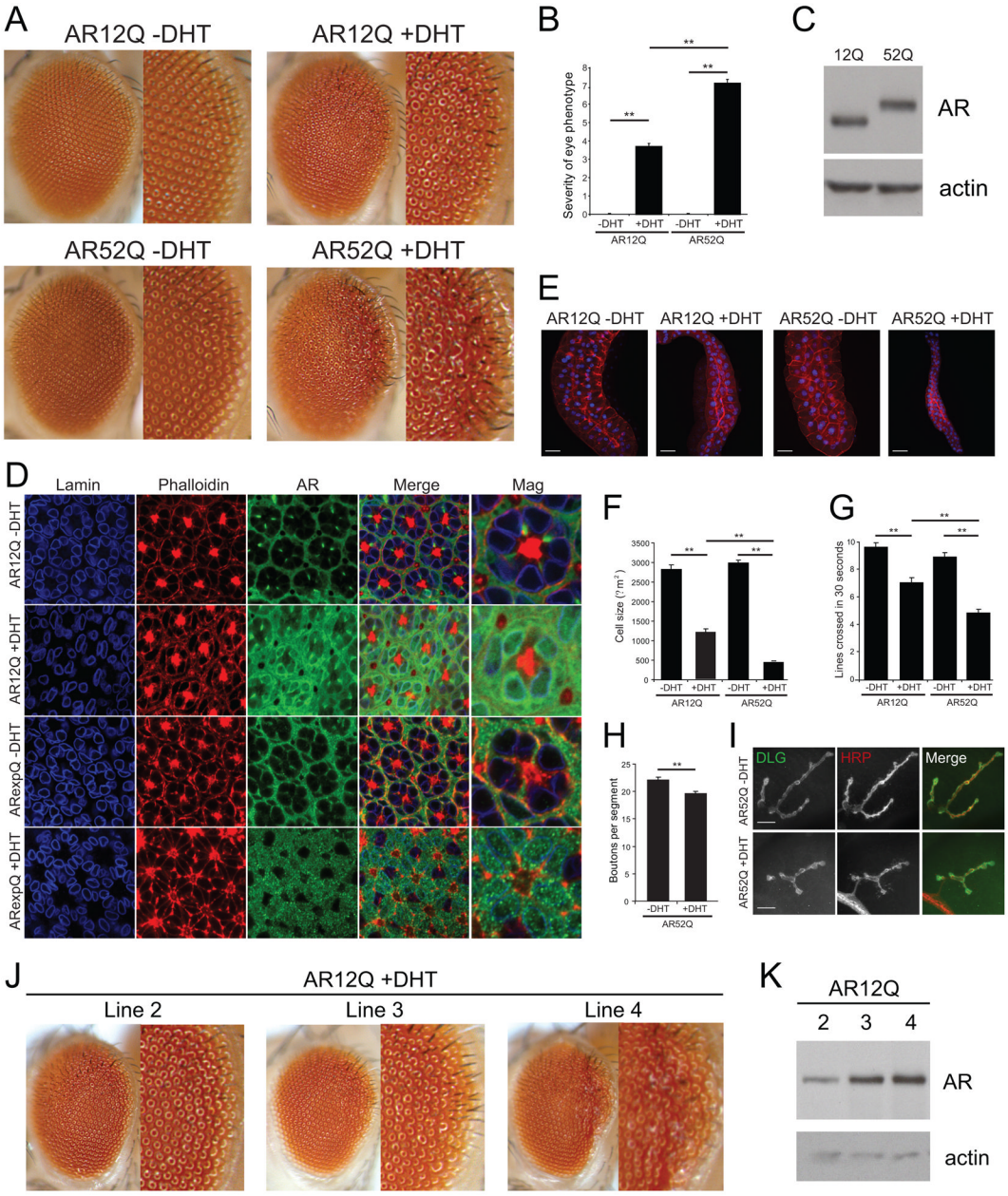

Figure 1. Expression of polyglutamine-expanded AR in *Drosophila* results in toxicity

(A) *Drosophila* females expressing AR in eyes using GMR-GAL4 were raised in medium containing vehicle or DHT and adult eye phenotypes were assessed by light microscopy. (B) Blinded scoring of the external eye phenotypes in (A) using a quantitative scoring system (Pandey et al., 2007). (C) Western blot showing levels of AR expression for AR12Q- and AR52Q-expressing flies shown in (A). (D) Pupae expressing AR in eyes using GMR-GAL4 were raised in medium with or without DHT and whole mount preparations of eye discs were immunostained for lamin (blue) and AR (green). Phalloidin (red) was used to stain F-actin. Samples were examined by confocal microscopy. (E–F) Third instar larvae expressing AR using the salivary gland fkh-GAL4 were dissected and stained with DAPI (blue) and phalloidin (red). Overall gland size shown in (E), cell size shown in (F). Phalloidin staining was used to delineate cell boundaries and determine cell size. Scale bar, 50 μm. (G) Third

instar larvae expressing AR12Q or AR52Q using D42-GAL4 were assessed for their ability to travel distances along the surface of an agar plate. (H–I) Larvae expressing AR52Q using OK371-GAL4 were raised in medium containing vehicle or DHT, dissected as third instar wandering larvae, and stained using the post-synaptic marker discs large (DLG, green) and the pre-synaptic marker HRP (red). Type 1B boutons were counted at muscle 4. Scale bar, 10 μm. (J) Female flies expressing AR12Q using GMR-GAL4 were raised on medium containing DHT. Each line shown represents an independent transformant line. (K) Western blot analysis of heads shown in (J). In (A) and (J), left side of each diptych shows light micrograph imaged at 63x, while right side shows increased magnification (~140x) of the posterior region of the eye in which degeneration is concentrated. ** $p<0.01$ in all panels. Bars, mean + SEM in all panels.

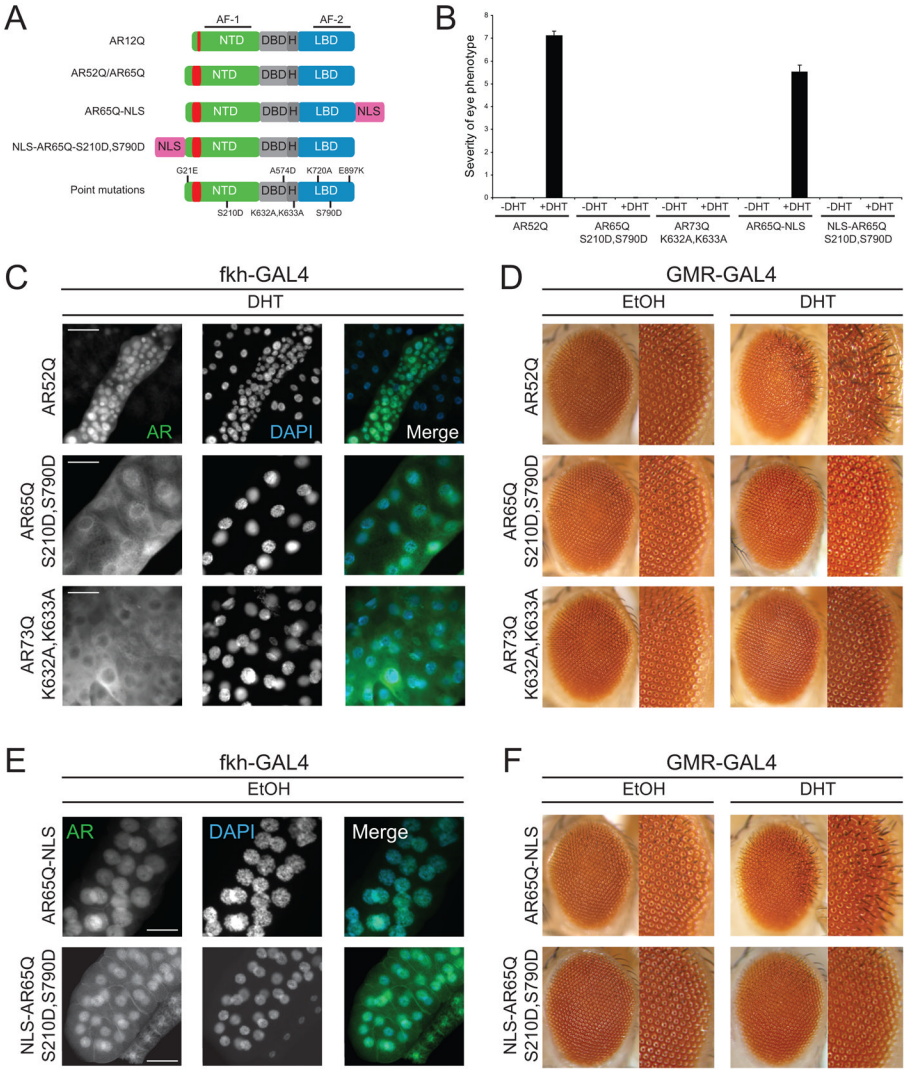

Figure 2. Nuclear localization of polyglutamine-expanded AR is necessary but not sufficient for toxicity *in vivo*

(A) Schematic of AR constructs used. NTD, N-terminal transactivation domain; DBD, DNA-binding domain; H, hinge; LBD, ligand-binding domain; NLS, nuclear localization sequence. (B) Blinded scoring of the external eye phenotypes in (D) and (F) using a quantitative scoring system. Bars, mean + SEM. (C) Salivary glands of *Drosophila* larvae expressing AR using fkh-GAL4. Larvae were raised in medium containing DHT and processed for immunocytochemistry. AR was detected with anti-AR antibody (green) and nuclei were stained with DAPI (blue). Scale bar, 50 μm. (D) *Drosophila* females expressing AR in eyes using GMR-GAL4 were raised in medium containing vehicle or DHT and adult eye phenotypes were assessed by light microscopy. (E) Salivary glands of *Drosophila* larvae expressing AR using fkh-GAL4. Larvae were raised in medium containing ethanol and processed for immunocytochemistry as in (C). Scale bar, 50 μm. (F) *Drosophila* females expressing AR in eyes using GMR-GAL4 were raised in medium containing vehicle or DHT and adult eye phenotypes were assessed by light microscopy. See also Figure S1 and S2.

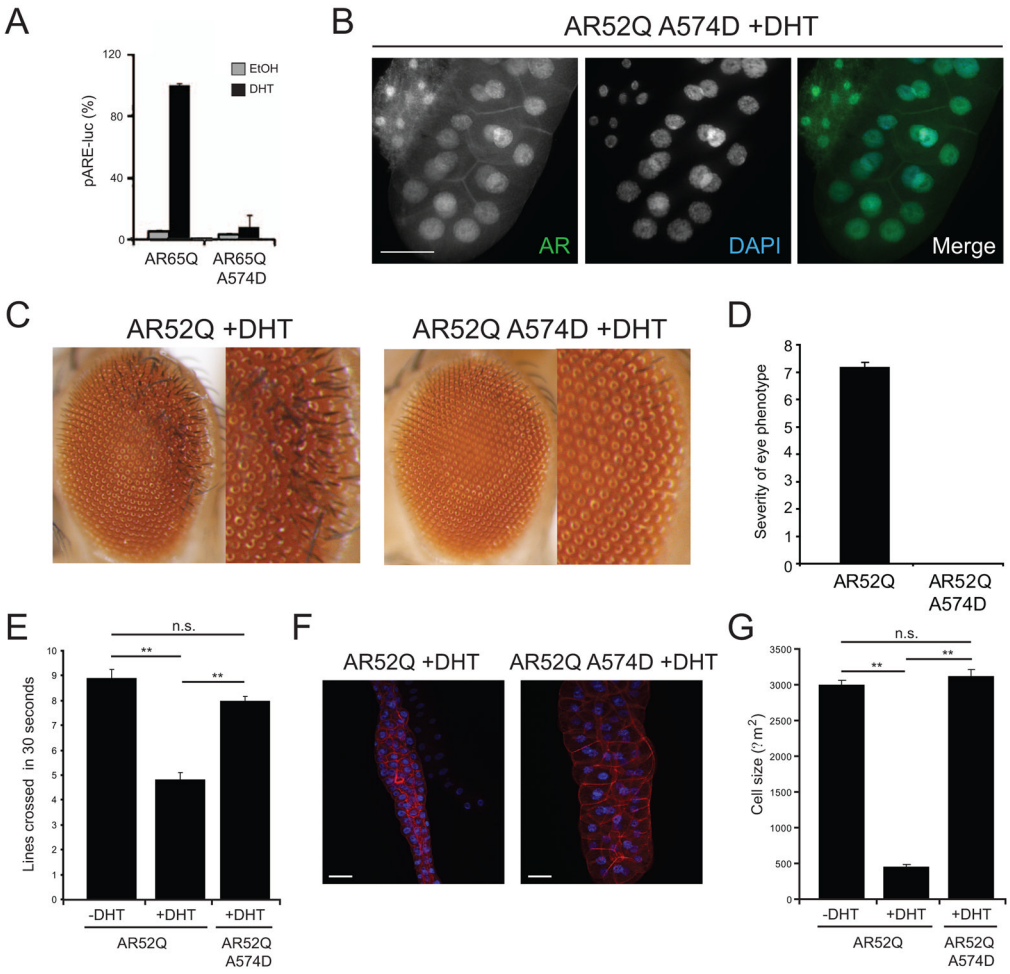

Figure 3. DNA binding by polyglutamine-expanded AR is required for toxicity

(A) HEK293T cells were transfected with indicated AR constructs together with both the luciferase pARE-E1b-Luc and the β-galactosidase pCMVβ reporter constructs. AR transactivation was measured in the presence and absence of DHT by luciferase assay and normalized to β-galactosidase activity. (B) Salivary glands of *Drosophila* larvae expressing AR using fkh-GAL4. Larvae were raised were raised in medium containing DHT and processed for immunocytochemistry. AR was detected with anti-AR antibody (green) and nuclei were stained with DAPI (blue). Scale bar, 50 μm. (C) *Drosophila* females expressing AR in eyes using GMR-GAL4 were raised in medium containing DHT and adult eye phenotypes were assessed by light microscopy. (D) Blinded scoring of the external eye phenotypes in (C) using a quantitative scoring system. (E) Third instar larvae expressing AR using the motor neuron driver D42-GAL4 were assessed for their ability to travel distances along the surface of an agar plate. (F–G) Third instar larvae expressing AR using the salivary gland fkh-GAL4 were dissected and stained with DAPI (blue) and phalloidin (red). Overall gland size shown in (F), cell size shown in (G). Phalloidin staining was used to delineate cell boundaries and determine cell size. Scale bar, 50 μm. ** $p<0.01$ in all panels. n.s., not significant. Bars, mean + SEM in all panels. See also Figure S2 and S3.

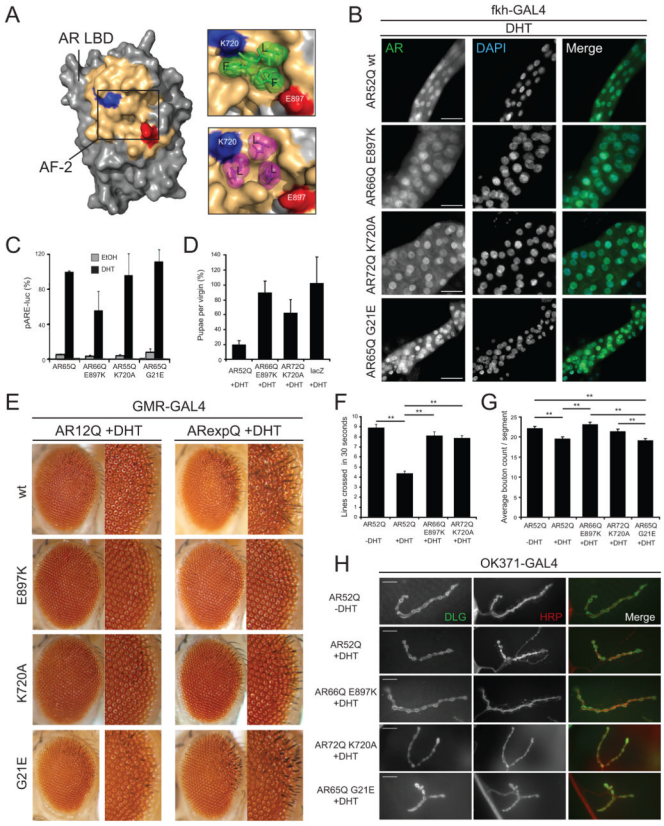

Figure 4. Disruption of AF-2 blocks polyglutamine-expanded AR toxicity

(A) Crystal structure of the AR LBD (PDB ID: 2AMA) showing the AF-2 binding surface (gold) and the two charge clamp residues in AF-2, K720 (blue) and E897 (red). Green, FxxLF peptide co-crystallized with AF-2 (PDB ID: 1T7R). Pink, LxxLL peptide co-crystallized with AF-2 (PDB ID: 1T7F). (B) Salivary glands of *Drosophila* larvae expressing AR using fkh-GAL4. Larvae were raised in medium containing DHT and processed for immunocytochemistry. AR was detected with anti-AR antibody (green) and nuclei were stained with DAPI (blue). Scale bar, 50 μm. (C) HEK293T cells were transfected with indicated AR constructs together with both the luciferase pARE-E1b-Luc and the β-galactosidase pCMV β reporter constructs. AR transactivation was measured in the presence and absence of DHT by luciferase assay and normalized to β-galactosidase activity. (D) Viability assay of *Drosophila* expressing indicated AR transgenes using elav-GAL4. Crosses were performed in medium containing DHT. The number of pupae from each 1×1 cross was counted and normalized to lacZ. Expression of AR52Q resulted in larval lethality, while E897K or K720A mutations increased survivability to the pupal stage. (E) *Drosophila* females expressing AR in eyes using GMR-GAL4 were raised in medium containing DHT and adult eye phenotypes were assessed by light microscopy. Left, AR constructs with 12Q. Right, AR constructs with expanded Q (AR52Q wt, AR66Q E897K, AR72Q K720A, AR65Q G21E). See Figure S5E for phenotype severity scores. (F) Third instar larvae expressing AR using the motor neuron driver D42-GAL4 were assessed for their ability to travel distances along the surface of an agar plate. (G–H) Larvae expressing AR using the motor neuron driver OK371-GAL4 were raised in medium containing vehicle or DHT, dissected as third instar wandering larvae, and stained using the post-synaptic marker discs large (DLG, green) and the pre-synaptic marker HRP (red). Type 1B boutons were counted at muscle 4. Scale bar, 10 μm. ** $p<0.01$ in all panels. Bars, mean + SEM in all panels. See also Figure S2 and S5.

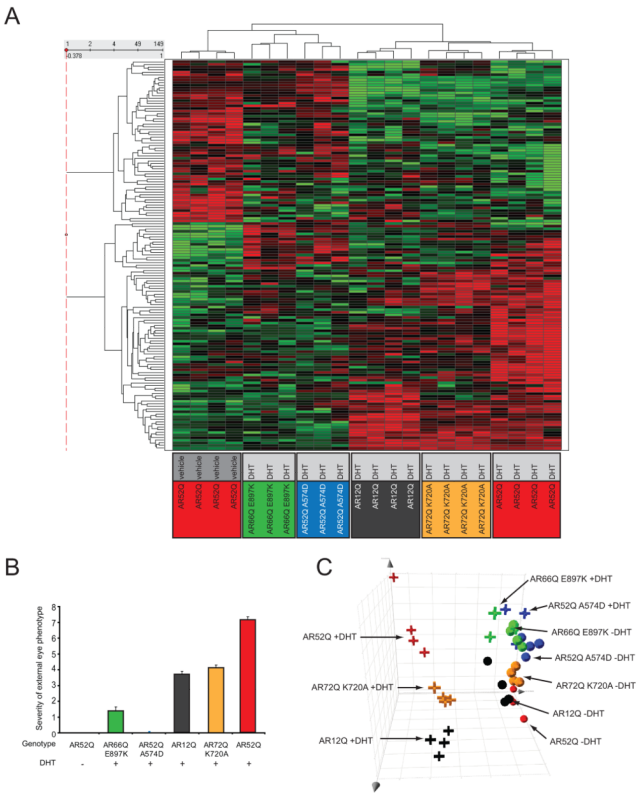

Figure 5. Molecular phenotype of AR mutants

(A) RNA from fly heads expressing AR using GMR-GAL4 was extracted and analyzed using Affymetrix arrays. Using a false discovery rate of 0.1, 149 genes were identified as showing significant changes in AR52Q flies due to DHT treatment and were thereby selected for further analysis. (B) Scoring of the external eye phenotype shows a correlation between the severity of the observable external phenotype and the clustering results. (C) PCA analysis using the 149 genes shown in (A). See also Figure S6 and Table S1.

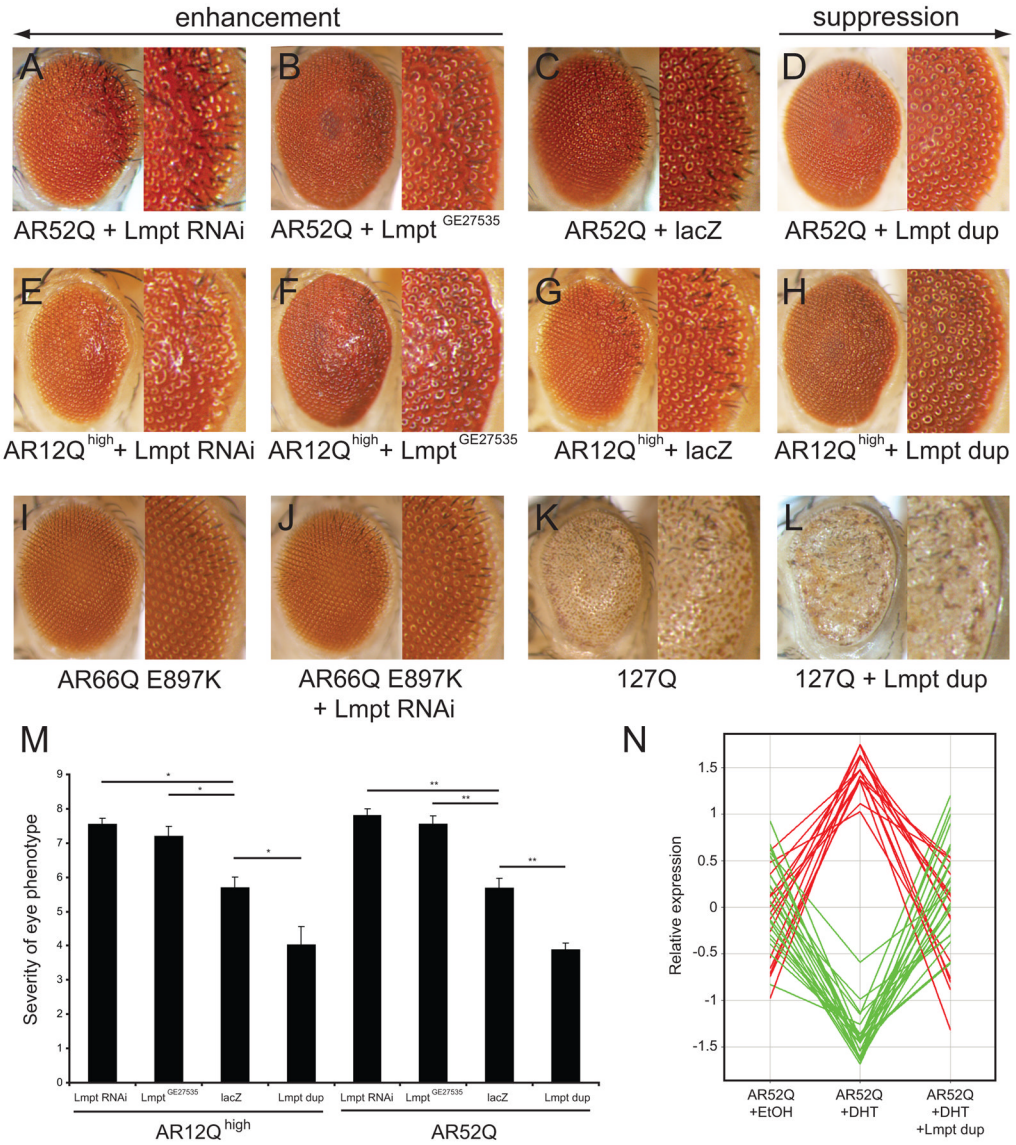

Figure 6. Manipulation of *limpet* levels modifies polyglutamine-expanded AR toxicity in an AF-2-dependent manner

(A–D) RNAi knockdown of limpet (A) and a P-element allele of limpet (limpet^{GE27535}) (B) enhance the phenotype of AR52Q alone (C). Flies with a chromosomal duplication of a region containing *limpet* (Dp(3;3)st^{+}g18) (D) show suppression of the AR52Q degenerative phenotype. (E–H) Limpet alleles similarly modify the phenotype of AR12Q flies with a strong phenotype. (I–J) Expression of limpet RNAi fails to enhance the phenotype in flies expressing AR66Q E897K. (K–L) Chromosomal duplication of *limpet* fails to suppress the phenotype in flies expressing pure polyglutamine (127Q). (M) Blinded scoring of the external eye phenotypes in (A–H) using a quantitative scoring system. All crosses performed on medium containing DHT. Bars, mean + SEM. ** $p<0.01$, * $p<0.05$. (N) Of 81 genes that changed in a DHT-dependent manner by expression profile analysis, 37 genes showed an opposite change in the presence of *limpet* duplication. Expression changes of these 37 genes are shown and plotted as relative expression (std dev) to the mean. See also Figure S7.

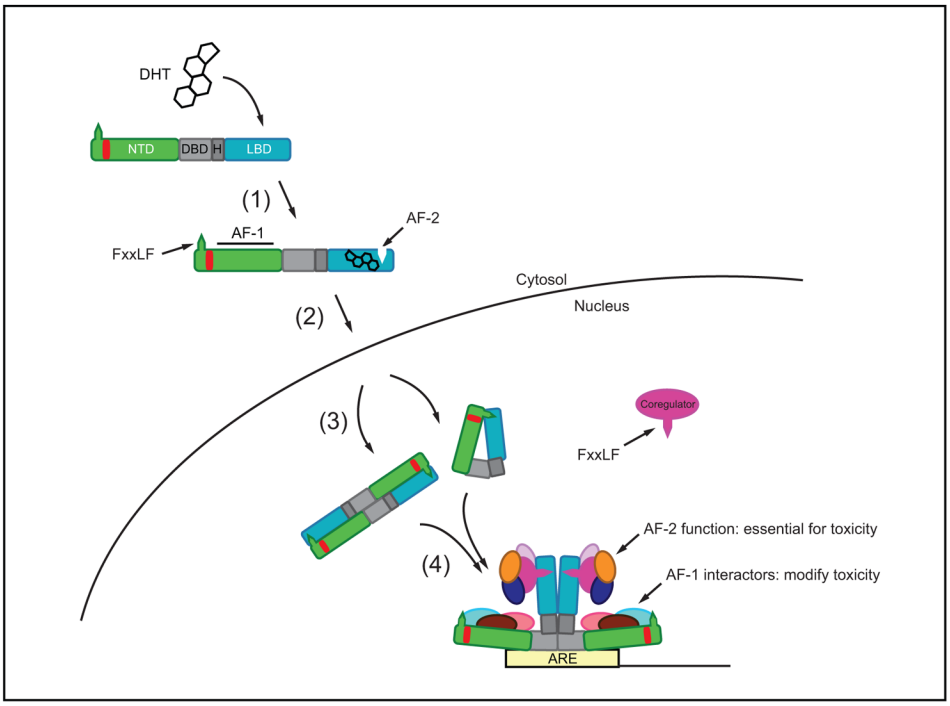

Figure 7. Schematic representation of the minimal ligand-dependent events that precede initiation of pathogenesis

(1) Ligand binding induces a conformational change in the LBD to create the AF-2 binding surface. Ligand also induces post-translational modifications that are not depicted. (2) Ligand-activated AR translocates to the nucleus. (3) Prior to DNA binding, the AF-2 domain is occupied by the N-terminal FxxLF in an intra- or inter-molecular interaction. (4) Following DNA binding, AF-1 and AF-2 interact with coregulators. In order to initiate pathogenesis, polyglutamine-expanded AR must bind DHT, translocate to the nucleus, bind DNA, and interact with coregulators at AF-2. While interactions at AF-1 modify toxicity, AF-2 function is essential for toxicity.

Table 1

Results from RNAi-based targeted genetic screen

73 previously described AR coregulator genes were investigated for the existence of *Drosophila* orthologs. We identified 61 putative orthologs and obtained RNAi lines for these genes from the Vienna *Drosophila* RNAi Center. RNAi lines were tested for their ability to modify the SBMA fly phenotype. Shown are 19 hits from the screen which dominantly modified the AR52Q eye phenotype. Mammalian orthologs and mechanisms of AR interaction are shown. As indicated, seven of these hits were found to have AF-2-based interactions. These seven hits were validated in motor neurons by larval crawling assay, as well as with alternate alleles (classical alleles or aneuploid aberrations) in the eye. See also Figure S4.

Hit from screen	Putative AR ortholog	Mechanism of AR interaction	AF-2-based interaction	Validation by alternate allele	Validation by larval crawling	Ref
CycD	CCND1	CCND1 decreases AR NTD/AF-2 interaction	X	Df enhances	enhances, p<0.05	(Burd et al., 2005)
Dif	RELA	RELA competes for AR coactivators				(Palvimo et al., 1996)
Dl	RELA	RELA competes for AR coactivators				
Ets96B	ETV5	ETV5-AR interaction represses metalloproteinase expression				(Schneikert et al., 1996)
Fkh	FOXH1	FOXH1 blocks DHT-induced AR nuclear foci				(Chen et al., 2005)
Groucho	AES	AES interacts with basal transcriptional machinery				(Yu et al., 2001)
gskt	GSK3B	GSK3B decreases AR NTD/AF-2 interaction	X	Df enhances	enhances, p<0.05	(Wang et al., 2004b)
Hey	HEY1	HEY1 represses AR AF-1				(Belandia et al., 2005)
Hr78	NR2C2	NR2C2 forms heterodimer with AR				(Lee et al., 1999)
Usp	NR2C2	NR2C2 forms heterodimer with AR				
jbug	FLNA	FLNA decreases AR NTD/AF-2 interaction	X	Df enhances	enhances, p<0.05	(Loy et al., 2003)
Lmpt	FHL2	FHL2 increases AR transactivation in AF- 2-dependent manner	X	P-element enhances	enhances, p<0.01	(Muller et al., 2000)
Pat1	APPBP2	APPBP2 inhibits AR nuclear translocation				(Zhang et al., 2004)
Pten	PTEN	PTEN inhibits AR nuclear translocation, promotes AR degradation				(Lin et al., 2004)
Rad9	RAD9	RAD9 decreases N/C interaction, requires AF-2	X	Df enhances	lethal with AR52Q	(Wang et al., 2004a)
Rbf	RB1	RB1 increases AR transactivation				(Yeh et al., 1998)
Smox	SMAD3	SMAD3 interrupts AR-coactivator interactions				(Hayes et al., 2001)
Smr	NCOR1/2	NCOR1/2 decreases N/C interaction, requires AF-2	X	Df enhances	n.s.	(Liao et al., 2003)

Hit from screen	Putative AR ortholog	Mechanism of AR interaction	AF-2-based interaction	Validation by alternate allele	Validation by larval crawling	Ref
wts	LATS2	LATS2 decreases N/C interaction, requires AF-2	X	EMS mutation enhances	enhances, p<0.05	(Powzaniuk et al., 2004)